Available online at www.sciencedirect.com

ScienceDirect

Procedia Engineering 199 (2017) 3480–3485

Procedia Engineering

www.elsevier.com/locate/procedia

X International Conference on Structural Dynamics, EURODYN 2017

Wind-tunnel tests on the post-critical response of classical-flutter-based generators

Luca Pigolotti[a,*], Claudio Mannini[a], Gianni Bartoli[a]

[a] *CRIACIV/Department of Civil and Environmental Engineering, University of Florence, Florence 50139, Italy*

Abstract

Harvesting energy from two-degree-of-freedom flutter requires large-amplitude steady-state oscillations. Nevertheless, the post-critical behaviour of this aeroelasic instability is still an open issue. The present study attempts to improve its scientific understanding and to supply information for the design of more unstable solutions for energy-harvesting applications. In this framework, the energy extraction was simulated through additional damping in the transverse motion component. Then, the influence of some governing parameters was explored through wind-tunnel tests and parametric linear analyses. It was found that a small mass unbalance downstream of the elastic centre is fundamental to anticipate the instability and to obtain unstable systems also in the presence of high damping levels. Moreover, the still-air frequency ratio is the main responsible for the magnitude of the pitching-to-heaving amplitude ratio. An increment of the heaving damping significantly affects the motion amplitude and conditions the optimal position of the elastic axis. Finally, the post-critical response seems to be little affected by the flow turbulence, suggesting the high potentiality of flutter-based generators for applications in real-flow environments.

Peer-review under responsibility of the organizing committee of EURODYN 2017.

Keywords: Classical Flutter; Post-Critical Motion; Damping; Energy Harvesting; Turbulence; Wind-Tunnel Tests

1. Introduction

In the common practice of wind and aeronautical engineering, dynamic fluid-structure interaction is considered a dangerous phenomenon, and the design of structures usually focuses on limiting any flow-induced vibrations. However, several aeroelastic phenomena can arise when slender structures are excited to produce self-induced aerodynamic loads [1]. In some cases, nonlinear effects lead the system response to Limit Cycles of Oscillations (LCOs), exhibiting limited amplitudes in a range of flow velocities (*e.g.* vortex-induced vibrations), or unrestricted amplitudes with the flow velocity after a critical threshold (*e.g.* galloping and flutter).

From a different perspective, recent studies established the production of renewable energy from flow-induced vibrations, recovering the kinetic energy during large-amplitude LCOs through specific energy-conversion apparatus (*e.g.* [2]). The aero-/hydro-elastic generators considered so far are based on: vortex-induced vibrations (*e.g.* [3]); transverse (*e.g.* [4]) and torsional (*e.g.* [5]) galloping; wake-galloping (*e.g.* [6]); flapping (*e.g.* [7–9]) and fluttering

* Corresponding author. Tel.: +39-055-275-8858
E-mail address: luca.pigolotti@dicea.unifi.it

1877-7058
Peer-review under responsibility of the organizing committee of EURODYN 2017.
10.1016/j.proeng.2017.09.458

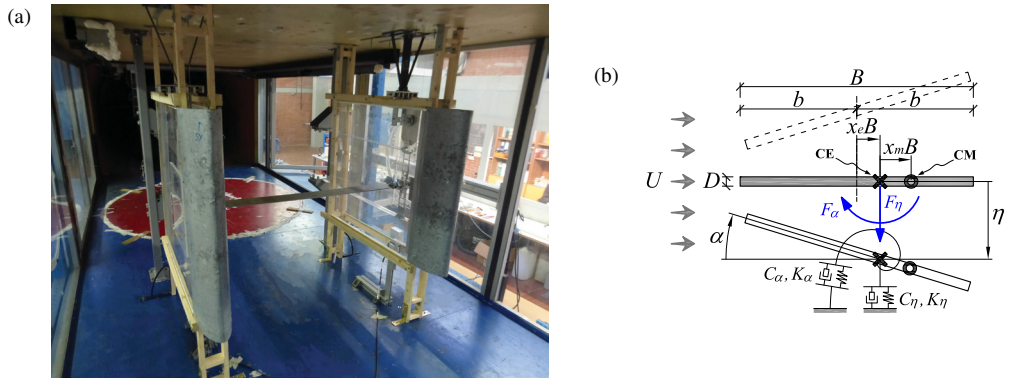

Fig. 1: (a) View of the aeroelastic setup in the wind tunnel; (b) schematic of the 2-DoF-flutter problem, being indicated some of the main parameters.

(*e.g.* [10]) wings. A systematic review of the state of the art can be found in [11,12]. Among all, the solutions involving a motion with two Degrees of Freedom (DoFs), such as flutter, seem to be the most promising (*e.g.* [9,10]).

Nevertheless, only few research studies have been conducted so far on the scientific understanding of the post-critical regime of flutter (*e.g.* [13,14]), despite this is fundamental for the design of flutter-based generators. Quasi-steady and semi-empirical approaches can be employed to approximate the system response (*e.g.* [15,16]), although reliable predictive models for the post-critical behaviour are still missing. Therefore, numerical CFD (*e.g.* [17, 18]) and experimental (*e.g.* [19,20]) investigations are often used, even though they require complex design of the computational and aeroelastic setups due to the large-amplitude motion.

The present study investigates the post-critical behaviour of 2-DoF flat plates prone to the classical-flutter instability. Linear analyses are performed to explore parametrically the critical condition, and extensive wind-tunnel tests are conducted to study the post-critical response. The main objective is to understand the influence of some of the governing parameters on the flutter-induced motion of systems simulating the operation of a power generator.

2. Methodology of investigation

The experimental campaign was conducted in the open-circuit wind tunnel of CRIACIV in Prato, Italy. An aeroelastic setup (Fig. 1a) was specifically designed to enable a large-amplitude motion with vertical (or heaving, η) and rotational (or pitching, α) components. The former was provided through a system composed by coil springs and flexible leaf-spring frames, while the latter by clock springs. The heaving damping was controlled through eddy-current-based magnetic dampers, and it was increased to simulate the presence of the energy-conversion apparatus. The steel model (Fig. 1a) had an elongated rectangular cross section with sharp edges, which was 100 mm wide (B) and 4 mm deep (D), the smaller dimension facing the wind. Two models were tested differing for the span length (l), namely 517 mm (configurations coded as `H`) and 1008 mm (coded as `L`). The model ends were connected to the elastic suspension through a device that allowed managing the eccentricity of the elastic centre (e, positive if downstream of the section midchord) and to add known masses to shift the mass-centre eccentricity (a, positive if downstream of the elastic axis). The operative Reynolds number was in the range 33,000 to 120,000 ($Re = UB/\nu$, with ν=0.15 cm^2/s). The mean flow speed U was measured by a Prandtl probe, installed upstream of the model, and then corrected through known flow maps to infer the velocity at the model centreline. The heaving motion component was recorded through analog laser displacement transducers, while two accelerometers were installed for the pitching component; the frequency sampling was 2000 Hz. Heaving displacements up to about a chord B and pitching rotations of about 90° were recorded during the tests. The maximum blockage ratio was about 6.25%, reached for rotations of 90°.

The two-dimensional flutter problem is illustrated in Fig. 1b, where the 2-DoF motion is described through $\eta(t) = \hat{\eta}e^{i\omega t}$ and $\alpha(t) = \hat{\alpha}e^{i(\omega t+\hat{\phi})}$, being $\omega = 2\pi n$ the circular flutter frequency. The well-known linear model of Theodorsen (not reported here for the sake of brevity) was applied to describe analitically the self-excited loads at the incipient instability [21]. Then, the dimensionless parameters that play a role in the flutter problem are the following:

$$\xi_{\eta 0} = \frac{C_\eta}{2\omega_{\eta 0} I_\eta}\,, \quad \xi_{\alpha 0} = \frac{C_\alpha}{2\omega_{\alpha 0} I_\alpha}\,, \quad x_e = \frac{e}{B}\,, \quad x_m = \frac{a}{B} = \frac{S}{I_\eta B}\,, \quad \mu = \frac{2I_\eta}{\rho B^2 l}\,, \quad r_\alpha = \sqrt{\frac{I_\alpha}{I_\eta B^2}}\,, \quad \gamma_n = \frac{n_{\alpha 0}}{n_{\eta 0}} \tag{1}$$

Table 1: Dynamic parameters of the configurations discussed in the paper (selected subset of a wider experimental campaign).

Code	ρ [kg/m^3]	I_η [kg]	I_α [kg m^2]	S [kg m]	$n_{\eta 0}$ [Hz]	$n_{\alpha 0}$ [Hz]	$\xi_{\eta 0}$ [%]	$\xi_{\alpha 0}$ [%]	x_e [−]	μ [−]	x_m [−]	r_α [−]	γ_n [−]	I_u [%]	L_u^x/B [−]
H1	1.15	8.06	0.032	0.073	1.89	1.82	0.05	1.67	0.00	2709	0.09	0.63	0.96	0.7	-
H3	1.24	7.87	0.032	0.045	1.73	1.81	0.04	1.24	"	2605	0.06	0.63	1.05	"	-
H6	1.16	"	0.029	0.000	"	1.90	0.05	1.23	"	2617	0.00	0.61	1.09	"	-
Hs1	1.17	7.88	0.032	0.031	1.73	1.81	0.04	1.24	0.00	2604	0.04	0.63	1.05	"	-
Hs4	"	"	"	"	"	"	4.62	"	"	2620	"	"	"	"	-
Hs4T1	"	"	"	"	"	"	"	"	"	2621	"	"	"	2.45	0.8
Hs4T2	"	"	"	"	"	"	"	"	"	2622	"	"	"	10.68	2.3
L19	1.22	8.53	0.021	0.048	1.98	1.82	0.05	0.75	−0.25	1392	0.06	0.50	0.92	0.7	-
L22	"	"	"	"	"	"	4.82	"	"	1422	"	"	"	"	-

being C_η and C_α the heaving and pitching damping coefficients, S the static mass unbalance, ρ the fluid density, I_η and I_α the heaving and pitching inertias, $n_{\eta 0} = \omega_{\eta 0}/2\pi$ and $n_{\alpha 0} = \omega_{\alpha 0}/2\pi$ the oscillation frequency of heaving and pitching motions, with $\omega_{\eta 0} = \sqrt{K_\eta/I_\eta}$ and $\omega_{\alpha 0} = \sqrt{K_\alpha/I_\alpha}$ (K_η and K_α are the heaving and pitching stiffness coefficients). Frequencies and damping coefficients refer to oscillations of the uncoupled systems (*i.e.* with $S = 0$) in still air. It is worth pointing out that the heaving damping ratio, $\xi_{\eta 0} = \xi_{\eta 0s} + \xi_{\eta 0e}$, comprises the mechanical damping $\xi_{\eta 0s}$ and the damping $\xi_{\eta 0e}$ added through the dampers, the latter being proportional to the energy flowing into the equivalent energy-conversion apparatus. Table 1 summarizes the governing parameters of the configurations discussed in the following, which represent a selected subset of a wider experimental campaign.

Tests were conducted in smooth flow, with a free-stream turbulence intensity I_u of about 0.7%. Then, two cases of homogeneous turbulence were also considered through the installation of bi-planar grids with two different sizes of the mesh, arranged at two different distances upstream of the model. In particular, I_u was about 2.45% and 10.67% in the two cases, and the longitudinal turbulence integral length scale L_u^x was, respectively, about $0.8B$ and $2.3B$.

3. Results

3.1. Numerical predictions of the instability threshold

The performance of a flutter-based generator can be strongly increased by reducing the critical flow speed [12], which is expressed in dimensionless form as either $U_R^c = U^c/nB$ or $U_{R\alpha}^c = U^c/n_{\alpha 0}B$. Therefore, linear analyses were carried out to explore the parametric space, looking for optimal configurations that show low values of U_R^c.

Key parameters to anticipate the instability are the position of the elastic centre (x_e) and of the mass centre (x_m). Fig. 2a shows the predictions of U_R^c in the $x_m - x_e$ space, for a value of the heaving damping of 9.52%. The presence of an optimal combination of these parameters is apparent, to which corresponds a global minimum, identified as $U_{R,opt}^c$. In particular, the lowest values of U_R^c lie on a deep valley well elongated in the x_e direction, indicating that a small mass unbalance $x_m \approx 0.06$ is able to foster significantly the instability. Fig. 2b shows that the optimal position of the elastic axis depends on the level of heaving damping, approaching the upstream quarter-chord for increasing $\xi_{\eta 0}$. Furthermore, low-damped configurations are much more sensitive to the still-air frequency ratio γ_n. In particular, for $\gamma_n > 1$ the system is more unstable when x_e is located close to the trailing edge.

Finally, also the inertial parameters, namely the mass ratio μ and the dimensionless polar-inertia radius r_α, importantly affect the system stability. The value $U_{R,opt}^c = 44.5$ in Fig. 2a was calculated for a system with $\mu = 2605$ and $r_\alpha = 0.63$ (values referring to the short-span model). In contrast, Fig. 2b predicts the response of systems having $\mu = 1400$ and $r_\alpha = 0.39$ (similar to the values obtained with the long-span model). In this case, values of $U_{R,opt}^c$ always lower than 30 are obtained for $\xi_{\eta 0} \approx 9.5\%$, indicating that lower-inertia systems are significantly more unstable.

3.2. Experimental investigation of the post-critical behaviour

The experiments allowed evaluating the influence of some governing parameters, mainly x_e, x_m, $\xi_{\eta 0}$ and γ_n (Table 1), on the post-critical response. For each configuration, different initial conditions were released for some flow

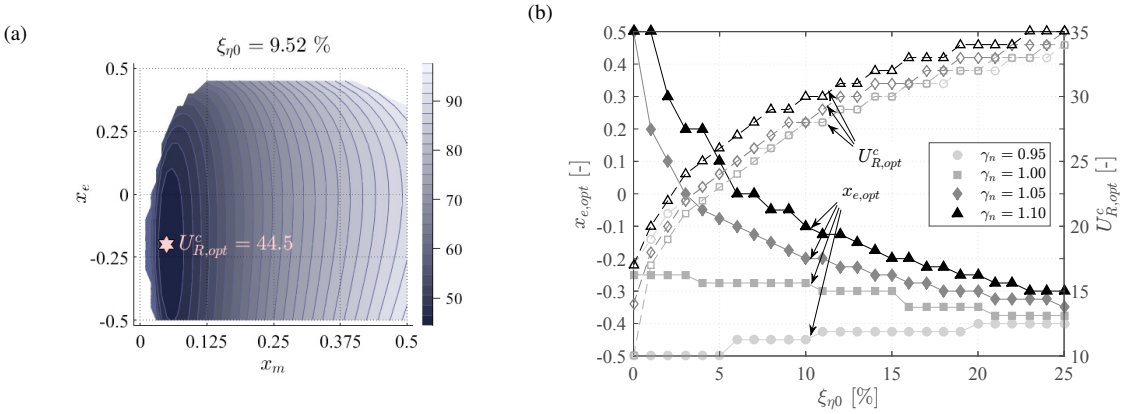

Fig. 2: (a) Example of critical-reduced-velocity map for a high-inertia system characterized by $\mu = 2605$ and $r_\alpha = 0.63$; (b) evolution with the heaving damping of $U^c_{R,opt}$ and corresponding optimal values of x_e, for a low-inertia system characterized by $\mu = 1400$ and $r_\alpha = 0.39$.

velocities close to the theoretical flutter boundary, in order to get information on the unstable branch position. Good agreement with the numerical predictions of the instability onset is found. The ensuing oscillation build up always comprises a transition regime, where the system adjusts its response to the nonlinear aeroelastic loads, which are due to the massive flow separation associated with the large-amplitude motion. The steady-state response is described in terms of the amplitude-velocity patterns of the heaving and pitching components, and by evaluating the oscillation frequency and the pitching-to-heaving phase shift. The system response was observed for increasing and decreasing flow speed, in view of the sub-critical bifurcation that was always found to characterise the flutter instability.

As predicted by the linear theory, the sole modification of x_m importantly anticipates the instability threshold (compare H3 and H6 in Fig. 3). Moreover, the region where lies the instantaneous centre of rotation of the model cross section moves from upstream to downstream of the midchord. Then, the pitching-to-heaving amplitude ratio is also very different. This motion parameter can be significantly affected by the still-air frequency ratio γ_n as well, as it is clear looking at the amplitude jump at the instability threshold (compare H1 and H3 in Fig. 3). Actually, in the case of $\gamma_n < 1$ (configuration H1), the heaving component is enhanced, and the centre of rotation lies in a small region downstream of the midchord, as suggested by the decrease of the phase angle $\hat{\phi}$ down to about $-164°$.

Fig. 4 shows the post-critical response of a few configurations with lower inertial parameters, namely L19 ($\xi_{\eta 0} = 0.05\%$) and L22 ($\xi_{\eta 0} = 4.82\%$), for which the elastic axis is located at the upstream quarter-chord ($x_e = -0.25$). The results are also compared to some test cases with both larger values of the inertial parameters and $x_e = 0$. It is clear that more unstable configurations can be designed by properly selecting the set of governing parameters, as indicated by the larger amplitudes of the motion of the lower-inertia systems. Moreover, the latter show a more prominent heaving component, which also has a positive impact for energy-harvesting purposes, since the conversion apparatus is supposed to act in that DoF.

As previously mentioned, the study of the heaving-damping influence is important to design flutter-based generators. In the case of the configurations reported in Fig. 4, increments of the heaving damping reduces the motion amplitude, and this occurs for both lower- and higher-inertia configurations. Nevertheless, a destabilizing effect of damping was observed in some cases, when γ_n was significantly larger that unity [20]. The increase of the heaving damping is also responsible for the modification of the motion phase toward a quadrature condition (Fig. 5), and the variations of the system response tend to saturate for very high values of $\xi_{\eta 0}$ [20]. However, even for high levels of heaving damping the amplitude-velocity paths preserve the same qualitative features, such as the sudden jump at the instability threshold and the drop-down at the lower bound of the subcritical branch, or the nearly linear evolution with the flow speed of the sub-critical and post-critical branches.

Finally, Fig. 4 highlights the response modifications induced by the increments of the turbulence intensity I_u. Comparing configurations Hs4, Hs4T1 and Hs4T2, all having $\xi_{\eta 0} = 4.62\%$, the motion amplitude is only slightly reduced even for the high-turbulence case with $I_u = 10.68\%$, and the system maintains a similar shape of the amplitude-velocity pattern. The effect of turbulence seems to be similar to that of damping, since it changes the phase of the motion toward the quadrature-phase (Fig. 5). Therefore, free-stream turbulence may be considered to act like a dissi-

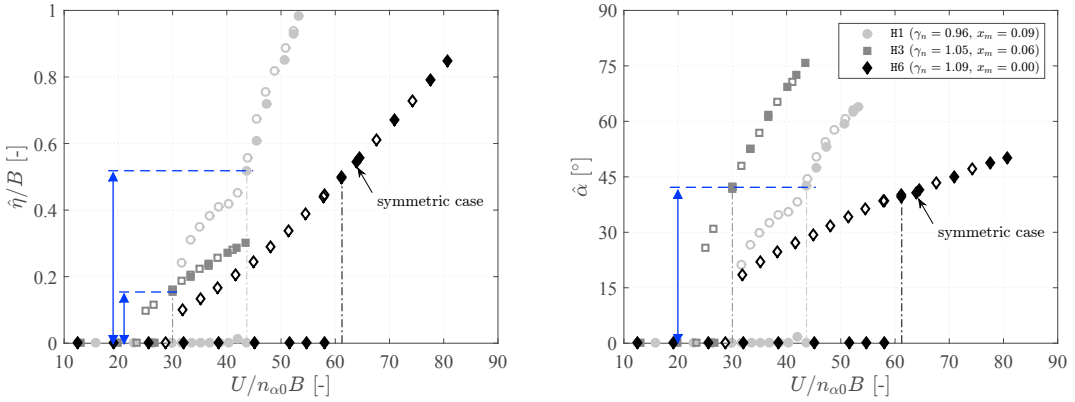

Fig. 3: Post-critical response for some high-inertia systems with $\xi_{\eta 0} \simeq 0.05\%$, for different mass-unbalance values and still-air frequency ratios.

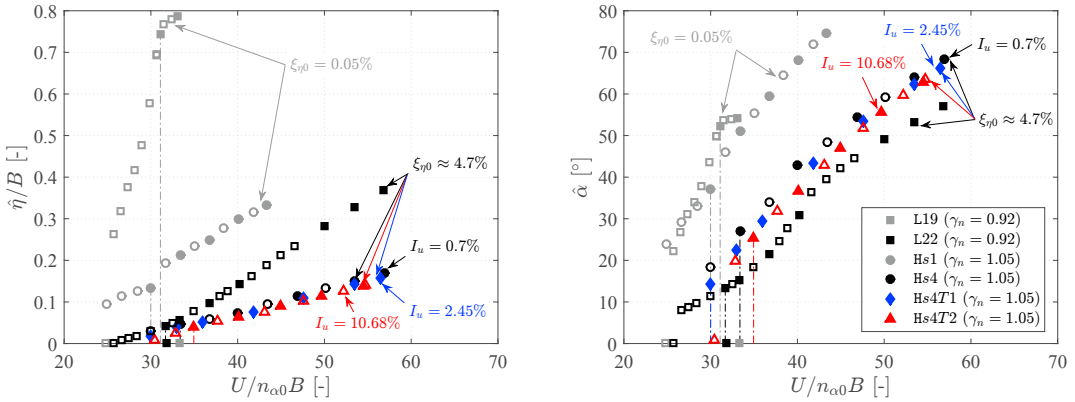

Fig. 4: Post-critical response for high- and low-inertia systems for different levels of heaving damping and turbulence intensity.

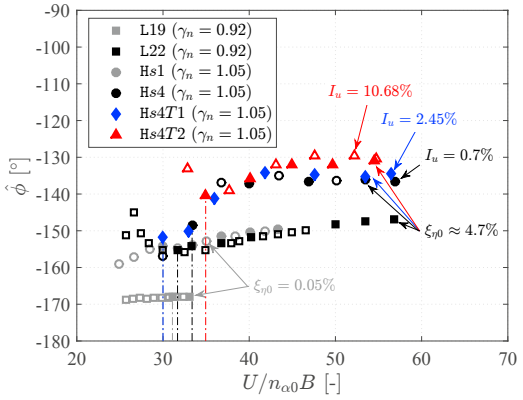

Fig. 5: Post-critical patterns of the pitching-to-heaving phase $\hat{\phi}$ for the systems of Fig. 4.

pation mechanism in the transfer of the aerodynamic loads to the structure [21]. Furthermore, high levels of incoming turbulence may be sufficient to trigger the motion in the sub-critical range of flow speeds, enhancing the operative range of flutter-based generators in realistic wind-flow conditions.

4. Conclusions

The response of two-degree-of-freedom flat-plate models undergoing the classical-flutter excitation has been investigated through systematic wind-tunnel tests and linear analyses. The aim was both to improve the knowledge of flutter-induced motion and to provide some design guidelines for flutter-based generators.

The experimental flutter boundaries are in agreement with the numerical linear predictions, which also confirm that lighter system are more unstable. Reductions of the critical flow speed can be achieved moving the mass centre slightly downstream of the elastic centre, which is also a prerequisite to observe the instability in the case of high-damped systems. The optimal position of the elastic axis depends on the heaving-damping level, usually moving from the trailing edge to the upstream quarter-chord point as the damping is increased. The still-air frequency ratio also plays a key role, since it strongly affects the motion in terms of both pitching-to-heaving amplitude ratio and phase lag. Finally, with the aim to reproduce real-flow conditions, preliminary investigations in high-turbulence flows were also conducted, and it was found that self-sustained motion still occurs, with only a slight delay of the system response.

Acknowledgements

The authors wish to thank Mikel Ogueta Gutiérrez (from Polytechnic University of Madrid), Dr. Tommaso Massai and Dr. Antonino Maria Marra for the support during the tests.

References

[1] E. Simiu, R. H. Scanlan, Wind Effects on Structures: Fundamentals and Application to Design, New York: John Wiley & Sons, 1996.
[2] S. Roundy, On the effectiveness of vibration-based energy harvesting, Journal of Intelligent Material Systems and Structures 16 (2005) 809–823.
[3] M. M. Bernitsas, K. Raghavan, Y. Ben-Simon, E. Garcia, VIVACE (Vortex Induced Vibration Aquatic Clean Energy): a new concept in generation of clean and renewable energy from fluid flow, Journal of Offshore Mechanics and Arctic Engineering 130 (2008) 041101.
[4] A. Barrero-Gil, G. Alonso, A. Sanz-Andres, Energy harvesting from transverse galloping, Journal of Sound and Vibration 329 (2010) 2873–2883.
[5] G. Ahmadi, Aeroelastic wind energy converter, Energy Conversion 18 (1978) 115–120.
[6] H.-J. Jung, S.-W. Lee, The experimental validation of a new energy harvesting system based on the wake galloping phenomenon, Smart Materials and Structures 20 (2011) 055022.
[7] W. McKinney, J. DeLaurier, Wingmill: an oscillating-wing windmill, Journal of Energy 5 (1981) 109–115.
[8] K. Isogai, M. Yamasaki, M. Matsubara, T. Asaoka, Design study of elastically supported flapping wing power generator, in: International Forum on Aeroelasticity and Structural Dynamics, Amsterdam, 2003.
[9] B. Simpson, F. Hover, M. Triantafyllou, Experiments in direct energy extraction through flapping foils, in: Proceeding of the 18th International Offshore and Polar Engineering Conference, Vancouver, BC, Canada, 2008, pp. 370–376.
[10] M. Bryant, E. Garcia, Modeling and testing of a novel aeroelastic flutter energy harvester, Journal of Vibration and Acoustics 133 (2011) 011010.
[11] L. Pigolotti, On the flutter response of two-degree-of-freedom flat plates for energy harvesting applications, Ph.D. thesis, Dept. of Civil and Environmental Engineering, University of Florence, Italy, and Dept. of Architecture, Civil Engineering and Environmental Sciences, University of Braunschweig - Institute of Technology, Germany, 2016.
[12] L. Pigolotti, C. Mannini, G. Bartoli, K. Thiele, Critical and post-critical behaviour of two-degree-of-freedom flutter-based generators, Journal of Sound and Vibration (accepted).
[13] B. Lee, S. Price, Y. Wong, Nonlinear aeroelastic analysis of airfoils: bifurcation and chaos, Progress in Aerospace Sciences 35 (1999) 205–334.
[14] E. H. Dowell, D. Tang, Nonlinear aeroelasticity and unsteady aerodynamics, AIAA Journal 40 (2002) 1697–1707.
[15] C. W. Emory, Prediction of limit cycle oscillation in an aeroelastic system using nonlinear normal modes, Ph.D. thesis, Aerospace and Ocean Engineering, Virginia Polytechnic Institute and State University, Blacksburg, Virginia, 2010.
[16] G. Fragiskatos, Non-linear response and instabilities of a two-degree-of-freedom airfoil oscillating in dynamic stall, Master's thesis, Dept. of Mechanical Engineering, McGill University, Montreal, Canada, 1999.
[17] Z. Peng, Q. Zhu, Energy harvesting through flow-induced oscillations of a foil, Physics of Fluids 21 (2009) 123602.
[18] I. Fenercioglu, B. Zaloglu, J. Young, M. Ashraf, J. C. S. Lai, M. F. Platzer, Flow structures around an oscillating-wing power generator, AIAA Journal 53 (2015) 3316–3326.
[19] X. Amandolese, S. Michelin, M. Choquel, Low speed flutter and limit cycle oscillations of a two-degree-of-freedom flat plate in a wind tunnel, Journal of Fluids and Structures 43 (2013) 244–255.
[20] L. Pigolotti, C. Mannini, G. Bartoli, Destabilizing effect of damping on the post-critical oscillations of flat plates, Meccanica (2017). DOI: 10.1007/s11012-016-0604-y.
[21] Y.-C. Fung, An Introduction to the Theory of Aeroelasticity, Dover Publications, Inc., New York (US), 2008.